JOC The Journal of Organic Chemistry

pubs.acs.org/joc Article

Synthesis and Application of Constrained Amidoboronic Acids Using Amphoteric Boron-Containing Building Blocks

Harjeet S. Soor, Diego B. Diaz, Ka Yi Tsui, Karina Calvopiña, Marcin Bielinski, Dean J. Tantillo, Christopher J. Schofield, and Andrei K. Yudin*

Cite This: J. Org. Chem. 2022, 87, 94−102 Read Online

ACCESS | Metrics & More | Article Recommendations | Supporting Information

ABSTRACT: Amidoboronic acid-containing peptidomimetics are an important class of scaffolds in chemistry and drug discovery. Despite increasing interest in boron-based enzyme inhibitors, constrained amidoboronic acids have received little attention due to the limited options available for their synthesis. We describe a new methodology to prepare both α- and β-amidoboronic acids that impose restrictions on backbone angles. Lewis acid-promoted Boyer−Schmidt−Aube lactam ring expansions using an azidoalkylboronate enabled generation of constrained α-amidoboronic acid derivatives, whereas assembly of the homologous β-amidoboronic acids was achieved through a novel boronic acid-mediated lactamization process stemming from an α-boryl aldehyde. The results of quantum chemical calculations suggest carboxylate-boron coordination to be rate-limiting for small ring sizes, whereas the tetrahedral intermediate formation is rate limiting in the case of larger rings. As part of this study, an application of β-amidoboronic acid derivatives as novel VIM-2 metallo-β-lactamase inhibitors has been demonstrated.

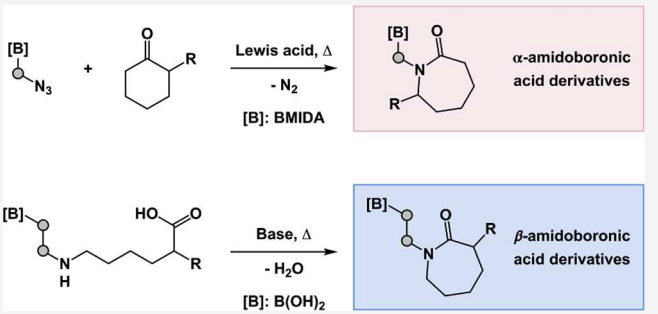

INTRODUCTION

Boron-containing peptides and small molecules are being increasingly used as biological probes and drugs. The use of boronic acids in these applications stems from boron's ability to interchange between sp^2 and sp^3 hybridization states and to reversibly react with heteroatom nucleophiles. In drug discovery, this covalent mode of action has led to the use of boron as an "electrophilic bait" for nucleophilic residues in enzyme targets such as proteasomes and β-lactamases.[1] The approval of several boron-based therapeutics, including bortezomib as a multiple myeloma drug and tavaborole as an antifungal agent, has encouraged the pursuit of methods to incorporate the boronic acid moiety into medicinally relevant heteroatom-rich scaffolds.[2−4] However, there has been comparatively little emphasis on conformationally constrained amidoboronic acid derivatives.[5−7]

Considerable synthetic efforts have been directed at controlling the conformation of peptidomimetics.[8,9] Many natural products including pencillins and related β-lactams belong to this class of molecules. Incorporation of *cis*-amides and heterocycles and introduction of bulky substituents into the peptide backbone have been used to exercise conformational control.[10,11] We recently reported that boron-containing molecules can engage with biological targets via a variety of coordination modes.[1] As part of this analysis, we found only a few cases that imposed conformational constraints around boron. Despite the success of boron-based therapeutics, synthetic technologies to site-selectively introduce boron into constrained heteroatom-rich environments remain underdeveloped. A possible reason for this lies in the thermodynamic preference of boron to form strong bonds with heteroatoms, limiting the palette of available synthetic options. With this challenge in mind, we became interested in developing mild synthetic approaches to assemble constrained boron-containing peptidomimetics.

Conformational control elements, such as cyclic diol-based ligands and boron-containing heterocycles, have been used to develop selective probes featuring relatively rigid frameworks (Figure 1A).[1] Kelly et al. reported that *N*-protected pyrroles can undergo a lithiation/borylation sequence followed by hydrogenation to afford saturated α-boroproline cores (Figure 1B).[12] Aggarwal et al. developed a photocatalytic methodology to access γ-boroproline derivatives via decarboxylative addition of amino acids to vinyl boronic acid derivatives (Figure 1C).[13] When it comes to biological application, the presence of the α-boroproline motif can be a hindrance since inhibitors are known to adopt cyclic motifs in solution through internal

Received: August 21, 2021
Published: December 13, 2021

https://doi.org/10.1021/acs.joc.1c02015
J. Org. Chem. 2022, 87, 94−102

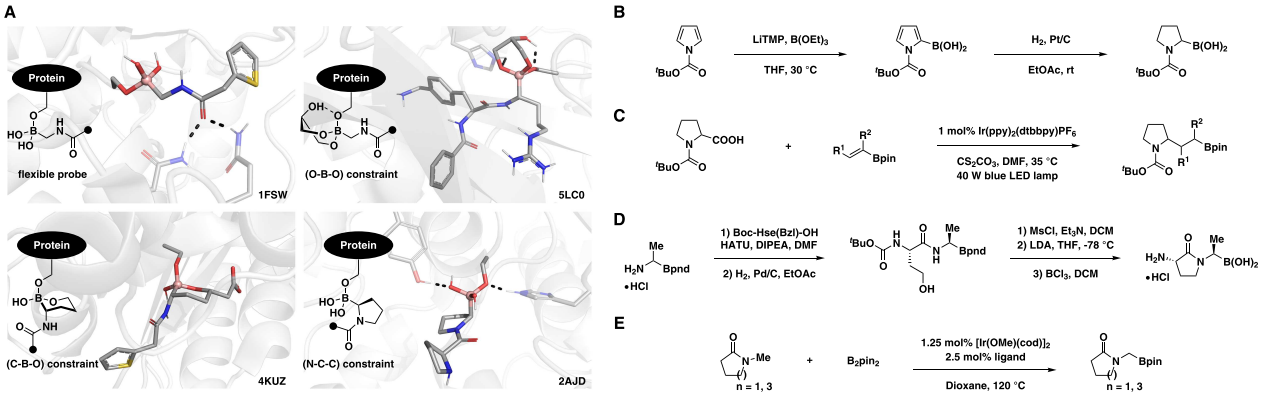

Figure 1. (A) Conformationally flexible and rigid boron-containing peptidomimetics bound to their corresponding hydrolase targets (AmpC, Zika virus NS2B-NS3, 4A5 Fab antibody, and dipeptidyl peptidase). (B) Lithium-borylation-reduction strategy of pyrroles to access well-documented α-boroproline motifs. (C) Decarboxylation and borylation enables access to a novel γ-boroproline scaffold. (D) α-Boro-proline motifs derived from cyclization of a homoserine-containing α-amidoboronic ester. (E) Directed C−H activation chemistry utilized to access a limited scope of α-amidoboronic acid derivatives.

amide coordination, interfering with the inhibitor mode of action. Tethering the boronic acid moiety to a nitrogen atom instead of carbon can prevent such interactions. This idea has been implemented in the synthesis of dipeptidyl peptidase inhibitors (Figure 1D);[14] chain extension between boron and the amide carbonyl avoided counterproductive internal coordination to boron. By employing directed C−H activation,[15] Clark et al. developed scaffolds where boron has a tether to nitrogen. However, this methodology provides mostly linear α-amidoboronic acid esters in moderate yields and with limited scope (Figure 1E). When it comes to constrained derivatives, only α-amidoboronic acids in five-membered boroproline motifs have been investigated. While variation in ring size[16] and homologation[17−19] strategies can modulate activity and selectivity of drug-like scaffolds, the available methodology does not allow for streamlined synthesis of constrained amidoboronic acids. Herein, we describe reactions that provide synthetic access to homologous BCN (boron−carbon−nitrogen) and BCCN (boron−carbon−carbon−nitrogen) motifs in various ring sizes. The BCN variants were synthesized by ring expansion of an *N*-methyliminodiacetic acid (MIDA)-protected azidoalkylboronate,[20] whereas constrained BCCN motifs[5,21−23] were accessed using a novel lactamization reaction that was inspired by native chemical ligation (NCL).[24]

RESULTS AND DISCUSSION

Previously, we investigated **1** as an intermediate towards the synthesis of covalent borofragments.[20] We hypothesized that Boyer−Schmidt−Aube lactam ring expansion of cyclic ketone **2** could afford α-amidoboronic acid derivative **3**.[25] Initial screening showed trifluoroacetic acid provided little selectivity and conversion being observed for the desired product, with several boron-containing species present, including boric acid. $Sc(OTf)_3$ led to high conversions, but lower selectivity (Table 1, entries 1 and 2), whereas $TiCl_4$ led to decomposition (entries 3 and 4). We found that the use of $BF_3{\cdot}OEt_2$ as a Lewis acid resulted in high conversion to **3a** in MeCN (entries 5−7). Use of acetonitrile as a solvent at elevated temperatures provided **3a** in good yield (entry 7).

The scale-up of **2a** yielded **3a** in a 73% isolated yield following normal-phase chromatography (Table 2). We found that a variety of boron-containing lactams could be obtained

Table 1. Reaction Condition Optimizations[a]

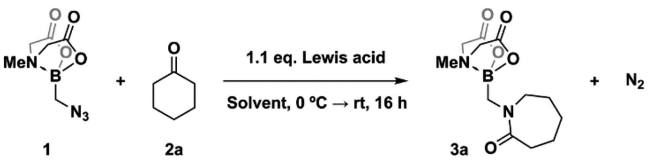

entry	Lewis acid	solvent	NMR yield (%)
1	$Sc(OTf)_3$	MeCN	<5
2	$Sc(OTf)_3$	DCM	0
3	$TiCl_4$	MeCN	<5
4	$TiCl_4$	DCM	0
5	$BF_3{\cdot}OEt_2$	MeCN	63
6	$BF_3{\cdot}OEt_2$	DCM	0
7[b]	$BF_3{\cdot}OEt_2$	MeCN	87

[a]Cyclohexanone (3.0 equiv) and Lewis acid (1.1 equiv) were added to an oven-dried 1 dram vial with an anhydrous solvent and cooled to 0 °C. Following dropwise addition of a solution of **1** (1.0 equiv), the reaction mixture was warmed to room temperature and stirred for 16 h. [b]Reaction was warmed to 50 °C.

from readily available ketones. Substituted ketones were eligible starting materials (**2b** and **2c**) and afforded derivatives **3b** and **3c**. The use of α,β-cyclohexenone enabled the formation of novel borylated enaminones **3d** through a formal [3 + 2] cycloaddition/ring contraction.[26] We explored the incorporation of the amidoboronic moiety into naturally occurring ketones and saw the formation of a ring-expanded steroidal derivative **3e**.[27] Our methodology was tolerant to different ring sizes, for example, ring expansion of cyclobutanone **2f** to furnish **3f** proceeded with excellent conversion. Deprotection under acidic and basic conditions led to decomposition. Having prepared the constrained α-amidoboronic acid derivatives, we sought to assess their potential biological activity.

Metallo-β-lactamases catalyze the hydrolysis of all β-lactam families including penicillins, cephalosporins, and carbapenems.[28] In contrast to nucleophilic serine-based broad spectrum β-lactamase inhibitors, there are as of yet no clinically useful inhibitors of zinc-dependent metallo-β-lactamases, which are of growing concern as a cause of antibiotic resistance.[29] However, they are known to be inhibited by some synthetically demanding bicyclic boro-

https://doi.org/10.1021/acs.joc.1c02015
J. Org. Chem. 2022, 87, 94−102

Table 2. Scope of Constrained α-Amidoboronic Acid Derivatives[b]

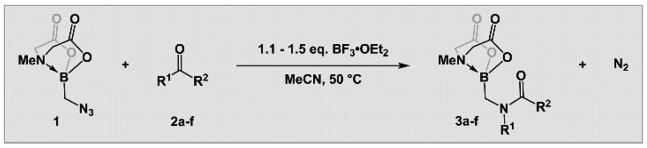

Cyclic ketone	Yield
2a cyclohexanone	3a (73%)
2b 2-methylcyclohexanone	3b (67%)
2c 2-phenylcyclohexanone	3c (55%)
2d[a] cyclohexenone	3d (45%, 1:1 *E/Z*)
2e androsterone	3e (56%)
2f cyclobutanone	3f (49%)

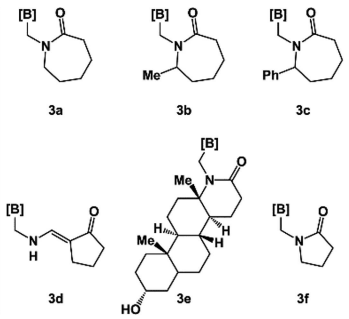

[a]**3d** was prepared by utilizing 3.0 equiv of cyclohexenone. [B] = BMIDA. [b]Reactions were performed using the optimized reaction conditions from Table 1 on 0.1−0.5 mmol scale at 0.2 M.

nates.[30] This challenge offers an opportunity to assess boron-based inhibitors that target metalloenzymes, yet they are structurally and mechanistically distinct from established boron-containing serine protease inhibitors.

We screened our constrained α-amidoboronic acids **3a−f** against a series of therapeutically relevant metalloenzymes. Compound **3a** displayed poor inhibitory values toward distinct metallo β-lactamases (see the SI for details). Although many boron-containing motifs that bind to enzymes are in a cyclic arrangement or adopt cyclic motifs before binding, there are some instances of straight-chain boronic acids that can engage protease targets. In these molecules, the chain length serves as a "ligand discrimination model".[31] We therefore wanted to explore the use of homologous β-amidoboronic acids as metalloenzyme inhibitors.

We surmised that β-aminoalkylboronic acids can potentially activate carboxylates intramolecularly toward lactam formation. This proposal resembles the mechanism of NCL in which a nucleophile such as cysteine/homocysteine targets a thioester with high chemoselectivity followed by S-to-N acyl transfer for amide formation.[24] We imagined that a "reversed polarity" ligation-type process could take place upon the attack by the carboxylate on electrophilic boron followed by B-to-N acyl transfer (Figure 2A).[32−36] We first were able to obtain a borylated lysine derivative **5a**. Upon treatment of **5a** with *N*,*N*-diisopropylethylamine (DIPEA) to neutralize any acid and elevated temperature, we saw complete conversion to **6a** (Figure 2B−D).

To probe the efficiency of this new cyclization, both modified and natural amino acid building blocks were employed, affording various five- and seven-membered lactam products (Figure 3A). Previously reported reductive amination and deprotection conditions allowed for the formation of linear precursors, which were then cyclized.[21] Purification using reverse-phase chromatography yielded constrained β-amidoboronic acids **6b−f** in good yields. The use of substituted α-borylaldehyde derivatives led to lactams with functionality next to boron. Efforts to increase the reaction scope led us to the synthesis of β-aminoboronic acid **7** through copper-catalyzed borylation of dehydroalanine.[37] The resulting scaffolds also underwent cyclization to provide **8a−d**.

We turned our attention to understanding the reaction mechanism. Density functional theory (DFT) calculations were performed using GAUSSIAN09.[38] Optimizations (without geometrical constraints) and frequency calculations for all intermediates and transition state structures (TSS) were performed at the CPCM(DMSO)-B3LYP/6-31 + G(d,p),[39,40] CPCM(DMSO)-M06-2X/6-31+G(d,p),[41] and CPCM-(DMSO)-ωB97XD/6-31+G(d,p)[42] levels of theory. The identity of each TSS was confirmed by examination of its imaginary frequency and using intrinsic reaction coordinate (IRC) calculations.[43] Conformational analyses were performed on all structures with SPARTAN10.[44] Multiple systematic search runs were performed with a molecular mechanics force field on all flexible torsions of each structure. Theoretical natural abundance ^{13}C kinetic isotope effects (KIEs) were simulated using KINISOT.[45] KIE values were predicted using the Bigeleisen and Mayer method.[46]

Our working mechanism (for the overall neutral system) starts with an intramolecular coordination of the boronic acid to the amide carbonyl to form **I** followed by dehydration to afford an active boronic ester **II** (Figure 3B). Intramolecular attack on carbon by the amine nitrogen results in a tetrahedral intermediate **III**, which through solvent-assisted proton transfer leads to **IV**. We also considered the anionic version of such a mechanism (starting with a carboxylate rather than a carboxylic acid), but the predicted barrier for formation of **III** was not kinetically feasible (>40 kcal/mol; see the SI for details). These results suggest that protonation prior to formation of **III** is necessary (see the SI for details). In the case of **5f**, we found that **TS0** was rate-limiting due to unfavorable torsional strain to form the active boronic ester (Figure 3B). This barrier toward boron coordination was much lower for **5a**, which suffers from less strain than **5f**.[47,48]

Active boronic ester **II** is predicted to be able to form tetrahedral intermediate **III** in both cases, with **5a** having a larger barrier. **III** was predicted to be slightly higher in free energy (but not electronic energy) than **TS2** for both cases, suggesting that this process can occur through a concerted asynchronous nucleophilic attack and proton transfer. Dehydration can then occur to generate the product.

With the developed methodology for creating classes of constrained β-amidoboronic acids, we wanted to evaluate their inhibitory potential. Metallo-β-lactamase inhibitory activity was measured by monitoring the fluorescence after enzymatic hydrolysis of the cephalosporin reporter molecule FC5 as reported.[49] Clinically relevant metallo-β-lactamases (VIM-1, 500 pM; NDM-1, 20 pM; VIM-2, 100 pM; IMP-1, 20 pM) were incubated for 10 min with different concentrations of the inhibitors (100 μM−5 nM) in MBL buffer (50 mM HEPES, pH 7.2, 1 μM $ZnSO_4$, 1 μg mL^{-1} BSA, 0.01% v/v Triton X-100). After incubation, the reporter FC5 (measured concentration: 5 μM) was added and hydrolysis was recorded using a ClarioStar or PHERAstar FS microplate reader (BMG LabTech). Captopril, a known binder of metallo-β-lactamases, was used as a positive inhibitor control. Constrained α-amidoboronic acid **3a**[22] was shown to be an ineffective MBL inhibitor, while **6b** was shown to have greater inhibition. **6b** was shown to inhibit VIM-1 and VIM-2 with IC_{50} values comparable to captopril. **6d** showed mild inhibition of both NDM-1 and VIM-2, while **8a** only showed inhibition of NDM-1. We turned our attention to understanding factors governing

https://doi.org/10.1021/acs.joc.1c02015
J. Org. Chem. 2022, 87, 94−102

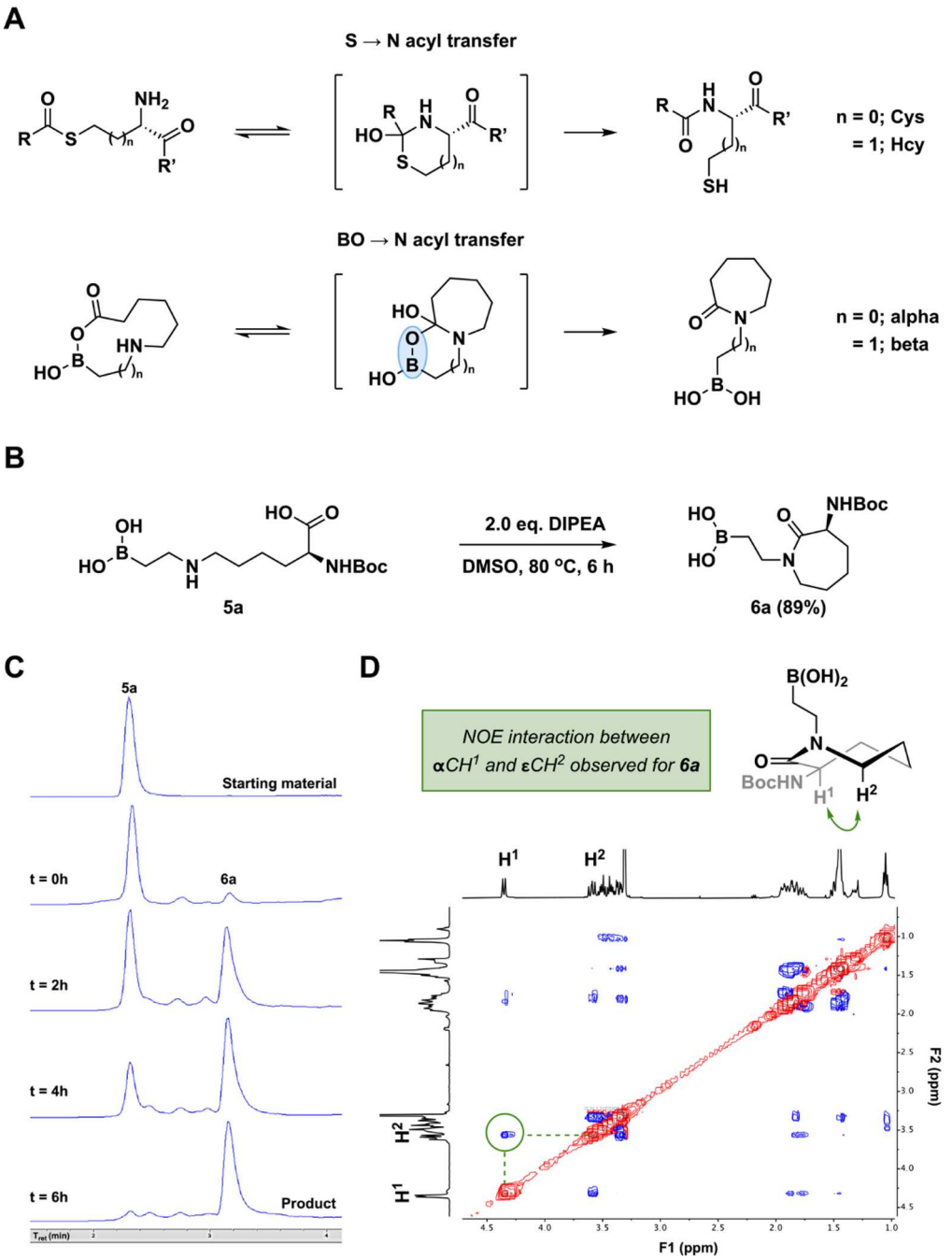

Figure 2. (A) Comparison of NCL and boron-mediated acyl transfers, where S-to-N and B-to-N acyl transfers are key steps. (B) Boron-mediated lactamization. Conditions: **5a** was dissolved in DMSO and heated. (C) Reaction monitoring using LC–MS at 80 °C. (D) 2D NOESY NMR evidence for cyclized product **6a** shows a correlation between H^1 and H^2, which is not observed in **5a**.

binding of **6b** to metalloenzyme VIM-2. Compound **6b** had an IC_{50} value of 7.9 μM against VIM-2. Boron-containing inhibitors typically react with hydrolytic residues rendering enzymes inactive.[50] Unlike typical nucleophilic serine β-lactamases, the metallo-β-lactamases employ a nucleophilic hydroxide stabilized by a bi-nuclear zinc complex.[51] Rather than reacting with a nucleophilic residue, boron-containing molecules inhibit metallo-β-lactamases by forming a boronate that mimics the tetrahedral intermediate in catalysis. The Fmoc group of **6b** may bind to a set of hydrophobic residues near the opening of the active site pocket (in an analogous manner to cephalosporin C-7 sidechain binding), along with additional hydrogen-bonding from water present near the pocket periphery.[52,53] The bulky lactam ring likely occupies a large pocket, forming hydrophobic contacts with nearby residues in much the same way the cyclic Captopril pyrrolidine ring interacts with the active site.[54] Compounds **6d** and **8a** displayed higher IC_{50} values than **6b**. **6d** is likely too bulky to bind efficiently as it has a substituent next to the boron center, which may bar entry into the active site. **8a** was substituent free; however, as the boronic acid moiety was in proximity of the ring system, it likely was not long enough to extend into the active site pocket. To the best of our knowledge, this is the first example of constrained β-amidoboronic acids binding to β-lactamase targets.

https://doi.org/10.1021/acs.joc.1c02015
J. Org. Chem. 2022, 87, 94–102

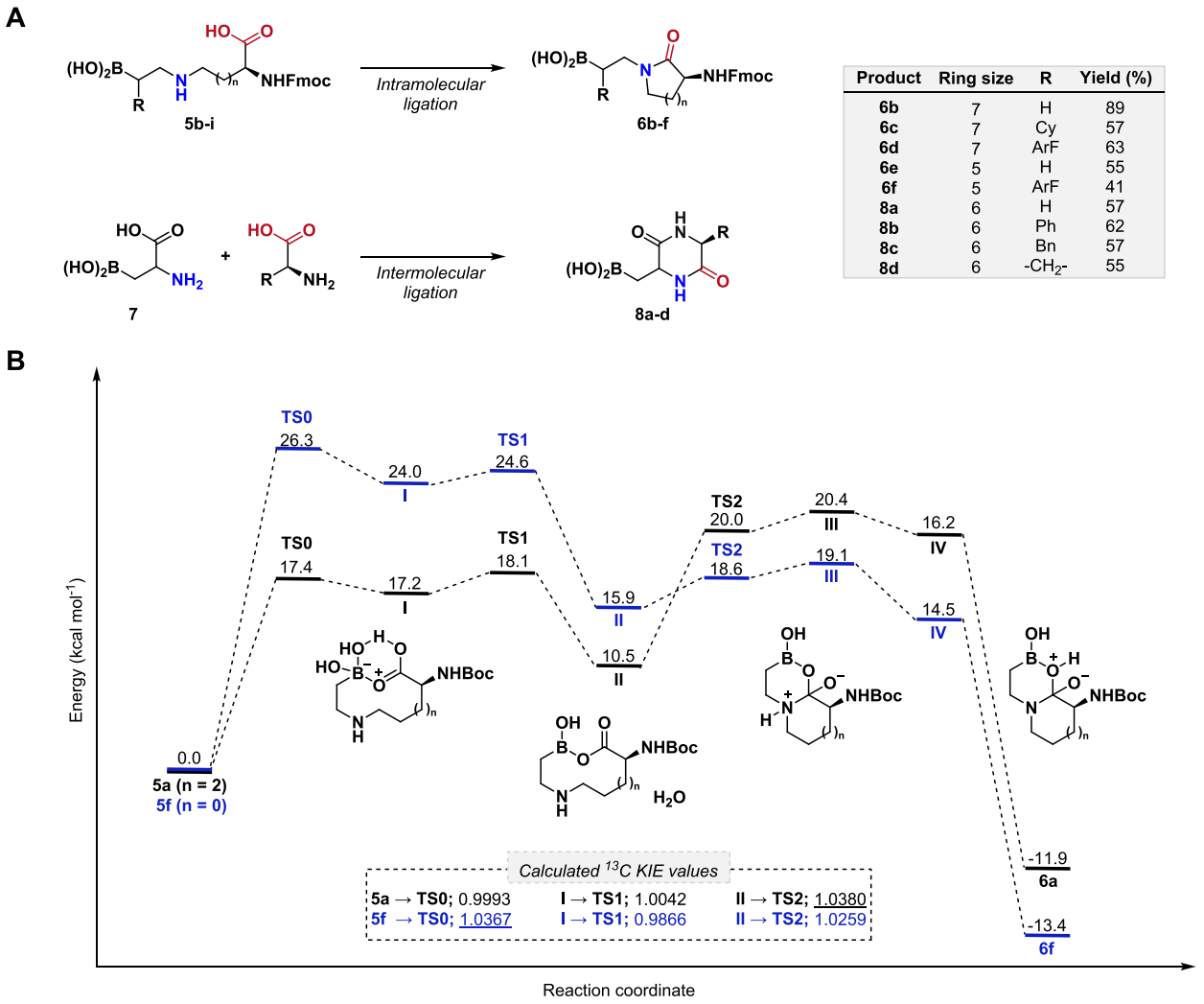

Product	Ring size	R	Yield (%)
6b	7	H	89
6c	7	Cy	57
6d	7	ArF	63
6e	5	H	55
6f	5	ArF	41
8a	6	H	57
8b	6	Ph	62
8c	6	Bn	57
8d	6	-CH_2-	55

Figure 3. (A) Scope of constrained boron-containing lactams displaying different ring sizes and substitutions. (B) Predicted pathways for formation of **6a/f**. Shown are free energies in kcal mol^{-1} calculated using CPCM(DMSO)-B3LYP/6-31+G(d,p). KIE values were calculated using KINISOT.

Despite the widespread use of linear boronic acid-based inhibitors, little work has been directed at modulating geometric constraints around the boron center. In this work, we implemented the synthesis of constrained α-amidoboronic acids through ring expansion using azidoalkylboronate **1**. This methodology allows the installation of relatively labile boronic acid moieties into a variety of heteroatom-containing scaffolds. An initial study of biological activity led us to pursue homologous β-amidoboronic acids through boron-mediated lactamization. Mechanistic insights suggested that the lactamization is sensitive to ring size, where the rate-limiting step is variable as a function of linker length. We have also uncovered that constrained β-amidoboronic acid derivatives such as **6b** are active against VIM-2, a therapeutically relevant metallo-β-lactamase. We anticipate that the new synthetic methodology will facilitate the rapid construction of a wide range of boron-containing inhibitors.

EXPERIMENTAL SECTION

General Information. Solvents were of reagent-grade quality and dried over 4 Å MS or distilled prior to use. Milli-Q water was used for reactions where needed. β-Aminoboronic acids[21−23] and α-azidoboronate[20] were synthesized according to previous protocols. ^{1}H NMR, ^{13}C NMR, and 2D NMR spectra were recorded on Varian Mercury 300, 400, or 500 MHz spectrometers. ^{11}B NMR spectra were recorded using Bruker 400/500 MHz spectrometers. For RP-HPLC/MS, low-resolution mass spectra (ESI) were collected on an Agilent Technologies 1200 series HPLC paired with a 6130 Mass Spectrometer. Compounds were resolved on a Phenomenex's Kinetex 2.6 μm C18 50 × 4.6 mm column at room temperature with a flow of 1 mL/min. The gradient consisted of eluents A (0.1% formic acid in double-distilled water) and B (0.1% formic acid in HPLC-grade acetonitrile). Different method types were used to analyze the compounds. For method A, a linear gradient started from 5% of B to 95% over 15 min at a flow rate of 1.0 mL/min. For method B, a linear gradient started from 5% of B to 95% over 4 min at a flow rate of 1.0 mL/min. It was kept constant at 95% for 1 min, and then returned to 5% over 0.5 min. For method C, it was kept constant at 5% of B for 0.5 min at a flow rate of 1.0 mL/min followed by a linear gradient to 95% over 5.5 min. It was kept constant at 95% of B for 0.5 min and then returned to 5% B over 0.5 min. High-resolution mass spectra were obtained on a VG 70-250S (double focusing) mass spectrometer at 70 eV or on an ABI/Sciex Qstar mass spectrometer with an ESI source, MS/MS, and accurate mass capabilities. Low-resolution mass spectra (ESI) were collected on an Agilent Technologies 1200 series HPLC paired to a 6130 quadrupolar mass spectrometer.

*General Procedure for Synthesis of Constrained α-Aminoboronic Acids (**3a−3f**).* To a flame-dried flask under a nitrogen atmosphere were added dry boryl alkyl azide (1 mmol, 1 equiv) and distilled MeCN (10 mL). The mixture was left to stir until the solution turned clear. Next, the carbonyl starting material (1.0−1.5

https://doi.org/10.1021/acs.joc.1c02015
J. Org. Chem. 2022, 87, 94−102

mmol, 1−1.5 equiv) was added down the side dropwise under a nitrogen atmosphere. After stirring until clear, $BF_3{\cdot}Et_2O$ was added dropwise into the solution either on ice or at room temperature depending on substrate solubility. The mixture was left to stir overnight. The solution was then quenched with brine and extracted 3 × 50 mL with EtOAc. The organic phase was then dried with $MgSO_4$, reduced under pressure, and dry loaded onto a column using Celite. The compounds were columned through a normal phase in gradients of Hex:EtOAc:MeCN.

General Procedure for the Synthesis of β-Aminoboronic Acids through Cu-Mediated Hydroboration. A mixture of dry CuCl (0.01 mmol, 5 mol %), KOtBu (0.03 mmol, 15 mol %), and 1,2-bis(diphenylphosphanyl)benzene (dppbz; 0.01 mmol, 5 mol %) in anhydrous THF (0.12 mL) was stirred for 30 min in a sealed tube under a nitrogen atmosphere. B_2pin_2 (0.26 mmol, 1.3 equiv) in THF (0.12 mL) was added. The reaction mixture was stirred for 10 min, and then the appropriate dehydropeptide (0.2 mmol, 1 eq.) in THF (0.12 mL) was added to the reaction mixture followed by MeOH (16 μL, 0.4 mmol). The reaction mixture was stirred at the room temperature for 20 h and filtered through a short plug of silica gel. The crude product was used for the following reaction without further purification. Note that the hydroboration products were unstable, so the purification operation should be quick.

*Synthesis of Constrained β-Aminoboronic Acids (**6b−6e** and **8a−8d**).* Aminoboronic acid was carried through from previous reports.[21−23] Aminoboronic acid (0.1 mmol, 1 equiv) was dissolved in 500 μL (0.5 M) of dry and sparged DMSO. Next, DIPEA (0.15 mmol, 1.5 equiv) was added to the solution and left to stir at 80 °C using an oil bath. Aliquots (at roughly 2 h intervals) were taken and subjected to LC−MS analysis. Upon completion, the solvent was removed under vacuum followed by lyophilization. The solid was then dissolved in a 1:1 mixture of MeCN and water. The solution was subjected to reverse-phase chromatography to yield the final product.

MIDA Group Deprotection. Different methods for the deprotection of the MIDA group were employed. In method I, in a 2 dram vial equipped with a magnetic stir bar and a screw-cap lid was dissolved β-amino (MIDA)-boronate (1.0 equiv) in THF (0.04 M). Then, 1.0 M NaOH(aq)(3.0 equiv) was added dropwise and the reaction mixture was stirred at room temperature for 30 min. The reaction was then quenched with a volume of phosphate buffer (pH = 7.0) equal to the volume of THF used. Et_2O was added, extracted, and separated. The aqueous layer was further extracted with a mixed solvent Et_2O:THF (1:1) (3 mL × 3). The organic phase was combined and concentrated to ∼1 mL. A 1:1 mixture of H_2O:MeCN was added and lyophilized to obtain white solids. In method II, in a 2 dram vial equipped with a magnetic stir bar and screw-cap lid was dissolved β-amino MIDA-boronate (1.0 equiv) in MeOH (0.04 M). $NaHCO_3$(s) was then added, and the reaction mixture was stirred at room temperature for 12 h while being monitored by LC−MS. The reaction was diluted with a volume of MeCN equal to the volume of MeOH used and filtered through a plug Celite while rinsing with MeCN. The crude product was adsorbed onto Celite from a solution of MeCN, purified by reverse-phase chromatography (H_2O:MeCN 95:5 to 5:95, with 0.1% formic acid), and then lyophilized to obtain white solids. In method III, in a 2 dram vial equipped with a magnetic stir bar and screw-cap lid was dissolved β-amino MIDA-boronate (1.0 equiv) in MeCN (0.1 M). A 3 M solution of HCl (aq)(6 equiv) made in H_2O was then added dropwise at room temperature, and the reaction was left to stir for 12 h while being monitored by LC−MS. Once quantitative MIDA deprotection was achieved, the crude product was adsorbed onto Celite and purified by reverse-phase chromatography and then lyophilized. Due to boronic acid proton exchange and boron's quadrupolar effect next to carbon, proton and carbon show discrepancy due to the absence in the NMR data compared to HRMS and molecular formula. Attempts to characterize single diastereomers occurred wherever possible. Moreover, discrepancies in nuclei, HRMS, and molecular formula can occur due to rotomer effects.

*4-Methyl-8-((2-oxoazepan-1-yl)methyl)dihydro-4l4,8l4-[1,3,2]oxazaborolo[2,3-b][1,3,2]oxazaborole-2,6(3H,5H)-dione (**3a**).* Reference amount: 0.1 mmol, 28 mg. White solid; 73% yield; ^{1}H NMR (400 MHz, CD_3CN) δ: 4.07 (d, *J* = 16.9 Hz, 2H), 3.94 (d, *J* = 16.9 Hz, 2H), 3.07 (t, *J* = 1.4 Hz, 3H), 2.89 (t, *J* = 18.7 Hz, 2H), 2.62 (m, 4H), 1.75−1.70 (m, 4H); ^{13}C{^{1}H} (101 MHz, CD_3CN): δ 168.6, 70.0, 63.0, 58.3, 45.2, 26.3; ^{11}B NMR (128 MHz, CD_3CN): δ 11.5; HRMS (DART-TOF) *m/z* [M + H]$^+$ calculated for $C_{12}H_{19}BN_2O_5$ = 283.1401, found = 283.1402.

*4-Methyl-8-((2-methyl-7-oxoazepan-1-yl)methyl)dihydro-4l4,8l4-[1,3,2]oxazaborolo[2,3-b][1,3,2]oxazaborole-2,6(3H,5H)-dione (**3b**).* Reference amount: 0.1 mmol, 30 mg. White solid; 67% yield; ^{1}H NMR (400 MHz, CD_3CN): δ 4.12 (d, *J* = 17.0 Hz, 2H), 4.00 (d, *J* = 17.0 Hz, 2H), 3.1 (t, *J* = 1.6 Hz, 3H), 2.69 (t, *J* = 18.4 Hz, 2H), 2.51 (m, 4H), 1.57−1.49 (m, 4H), 1.42 (m, 2H); ^{13}C{^{1}H} NMR (101 MHz, CD_3CN): δ 168.6, 63.6, 59.6, 56.2, 47.7, 24.3, 15.6; ^{11}B NMR (128 MHz, CD_3CN): δ 11.2; HRMS (DART-TOF) *m/z* [M + H]$^+$ calculated for $C_{13}H_{21}BN_2O_5$ = 297.1504, found = 297.1502.

*4-Methyl-8-((2-oxo-7-phenylazepan-1-yl)methyl)dihydro-4l4,8l4-[1,3,2]oxazaborolo[2,3-b][1,3,2]oxazaborole-2,6(3H,5H)-dione (**3c**).* Reference amount: 0.1 mmol, 36 mg. White solid; 55% yield; ^{1}H NMR (400 MHz, CD_3CN): δ 7.43 (s, 1H), 7.28 (s, 2H), 7.27 (s, 2H), δ 4.13 (d, *J* = 16.9 Hz, 2H), 3.95 (d, *J* = 16.9 Hz, 2H), 3.6 (s, 3H), 3.35 (m, 2H), 3.08 (t, *J* = 1.8 Hz, 3H), 2.94−2.80 (m, 2H), 2.60−2.54 (m, 2H), 2.11−2.02 (m, 2H), 1.84−1.75 (m, 3H); ^{13}C{^{1}H} NMR (101 MHz, CD_3CN): δ 168.7, 63.7, 62.8, 56.8, 47.7, 27.3, 26.6, 26.0, 25.4, 24.6; ^{11}B NMR (128 MHz, CD_3CN): δ 9.7; HRMS (DART-TOF) *m/z* [M + H]$^+$ calculated for $C_{18}H_{23}BN_2O_5H$ = 359.1792, found = 359.1793.

*(E)-4-Methyl-8-((((2-oxocyclopentylidene)methyl)amino)-methyl)dihydro-4l4,8l4-[1,3,2]oxazaborolo[2,3-b][1,3,2]-oxazaborole-2,6(3H,5H)-dione (**3d**).* Reference amount: 0.1 mmol, 28 mg. White solid; 45% yield; ^{1}H NMR (400 MHz, CD_3CN): δ 4.08 (d, *J* = 16.9 Hz, 2H), 3.96 (d, *J* = 16.9 Hz, 2H), 3.63−3.55 (m, 4H), 3.08 (t, *J* = 1.5 Hz, 3H), 2.74 (t, *J* = 18.7 Hz, 2H), 2.56−2.50 (m, 4H); ^{13}C{^{1}H} NMR (101 MHz, CD_3CN): δ 168.6, 67.4, 63.6, 62.4, 55.7, 47.8; ^{11}B NMR (128 MHz, CD_3CN): δ 10.2, used to obtain the ratio; HRMS (DART-TOF) *m/z* [M + H]$^+$ calculated for $C_{12}H_{17}BN_2O_5H$ = 281.2524, found = 281.2523.

*8-(((4aS,4bR,8R,10aS,10bS,12aS)-8-Hydroxy-10a,12a-dimethyl-2-oxohexadecahydronaphtho[2,1-f]quinolin-1(2H)-yl)methyl)-4-methyldihydro-4l4,8l4-[1,3,2]oxazaborolo[2,3-b][1,3,2]-oxazaborole-2,6(3H,5H)-dione (**3e**).* Reference amount: 0.1 mmol, 46 mg. White solid; 56% yield; ^{1}H NMR (400 MHz, DMSO-d_6): δ 4.16 (d, *J* = 3.0 Hz, 1H), 3.81 (p, *J* = 2.9 Hz, 1H), 2.37 (ddd, *J* = 18.9, 8.9, 1.1 Hz, 1H), 1.99 (dt, *J* = 19.0, 8.9 Hz, 1H), 1.89−1.69 (m, 2H), 1.67−1.37 (m, 8H), 1.37−1.07 (m, 9H), 0.76 (d, *J* = 8.0 Hz, 7H). ^{13}C{^{1}H} NMR(101 MHz, DMSO-d_6): δ 64.0, 54.0, 47.0, 35.6, 35.2, 34.5, 31.3, 30.5, 28.6, 21.3, 19.6, 13.4, 11.0. ^{11}B NMR (128 MHz, CD_3CN): δ 10.2; HRMS (DART-TOF) *m/z* [M + H]$^+$ calculated for $C_{25}H_{39}BN_2O_6H$ = 475.2901, found = 475.2901.

*4-Methyl-8-((2-oxopyrrolidin-1-yl)methyl)dihydro-4l4,8l4-[1,3,2]-oxazaborolo[2,3-b][1,3,2]oxazaborole-2,6(3H,5H)-dione (**3f**).* Reference amount: 0.1 mmol, 25 mg. White solid; 49% yield; ^{1}H NMR (400 MHz, CD_3CN): δ 4.29 (m, 4H), 3.04−2.95 (m, 2H), 2.29−2.21 (m, 2H), 1.85−1.77 (m, 3H), 1.77−1.68 (m, 4); ^{13}C{^{1}H} NMR (126 MHz, CD_3CN): δ 168.4, 137.9, 132.3, 130.6, 128.7, 127.5, 123.4, 62.4, 61.5, 59.5, 59.3, 46.7; ^{11}B NMR (128 MHz, DMSO-d_6): δ 9.9; HRMS (DART-TOF) *m/z* [M + H]$^+$ calculated for $C_{10}H_{15}BN_2O_5H$ = 254.1130, found = 254.1131.

*(S)-(2-(3-((((9H-Fluoren-9-yl)methoxy)carbonyl)amino)-2-oxoazepan-1-yl)ethyl)boronic Acid (**6b**).* Reference amount: 0.1 mmol, 42 mg. White solid; 89% yield; ^{1}H NMR (500 MHz, DMSO-d_6): δ 7.99−7.92 (m, 2H), 7.71−7.64 (m, 2H), 7.64−7.53 (m, 3H), 7.48−7.40 (m, 3H), 4.21−4.01 (m, 2H), 3.92 (b s, 2H), 3.80 (b s, 2H), 2.98 (s, 2H), 1.67 (s, 2H), 1.41 (s, 2H); ^{13}C{^{1}H} NMR (101 MHz, MeOD): δ 175.7, 169.9, 136.1, 130.5, 129.9, 128.6, 69.7, 69.4, 56.2, 44.1, 38.5. ^{11}B NMR (128 MHz, CD_3CN): δ 27.6; HRMS (DART-TOF) *m/z* [M + H]$^+$ calculated for $C_{23}H_{27}BN_2O_5H$ = 422.2018, found 422.2020.

*(2-((S)-3-((((9H-Fluoren-9-yl)methoxy)carbonyl)amino)-2-oxoazepan-1-yl)-1-cyclohexylethyl)boronic Acid (**6c**).* Reference amount:

https://doi.org/10.1021/acs.joc.1c02015
J. Org. Chem. 2022, 87, 94−102

0.1 mmol, 50 mg. Off-white solid; 57% yield; ^{1}H NMR (400 MHz, DMSO-d_6): δ 7.5 (s, 1H), 7.38−7.10 (m, 8H), 7.54 (m, 3H), 3.95−3.52 (m, 4H), 3.50−3.49 (m, 2H), 3.35−2.75 (m, 5H), 1.01 (m, 1H), 0.78, (m, 2 H), 0.5 (m, 2 H); ^{13}C{^{1}H} NMR (101 MHz, CD_3CN): δ 168.9, 168.8, 131.1, 129.2, 129.6, 127.7, 127.4, 126.1, 62.7, 46.8, 35.1. ^{11}B NMR (128 MHz, CD_3CN): δ 30.7; HRMS (DART-TOF) m/z [M + H]$^+$ calculated for $C_{29}H_{37}BN_2O_5H$ = 504.3002, found = 504.3001.

*(2-((S)-3-((((9H-Fluoren-9-yl)methoxy)carbonyl)amino)-2-oxoazepan-1-yl)-1-(4-fluorophenyl)ethyl)boronic Acid (**6d**).* Reference amount: 0.1 mmol, 52 mg. White solid; 63% yield; only the major isomer is reported; ^{1}H NMR (400 MHz, MeOD): δ 7.23−6.93 (m, 14H), 4.43 (hept, J = 6.6 Hz, 2H), 3.81 (t, J = 7.3 Hz, 2H), 3.69 (d, J = 17.1 Hz, 2H), 3.27 (s, 1H), 2.98 (dd, J = 13.9, 6.9 Hz, 1H), 2.85−2.73 (m, 1H). ^{13}C{^{1}H} NMR (151 MHz, CD_3CN): δ 168.9, 131.4, 129.6, 131.0, 129.7, 129.4, 128.4, 128.3, 128.2, 62.4, 49.6, 47.3; ^{11}B NMR (192 MHz, CD_3CN): δ 29.9; HRMS (DART-TOF) m/z [M + H]$^+$ calculated for $C_{29}H_{30}BFN_2O_5H$ = 516.2279 found = 516.2280.

*(S)-(2-(3-((((9H-Fluoren-9-yl)methoxy)carbonyl)amino)-2-oxopyrrolidin-1-yl)ethyl)boronic Acid (**6e**).* Reference amount: 0.1 mmol, 40 mg. Off-white solid; 55% yield; *major diastereomer characterized; ^{1}H NMR (600 MHz, DMSO-d_6); δ 7.93 (d, J = 7.5 Hz, 2H), 7.77−7.74 (br s, 2H), 7.52 (br s, 3H), 7.42 (s, 2H), 4.42 (s, 2H), 4.19 (s, 2H), 3.67−3.53 (m, 3H), 2.88 (s, 3H); ^{13}C{^{1}H} (126 MHz, DMSO-d_6): δ 134.0, 133.8, 132.4, 130.1, 128.8, 125.9, 60.0, 55.7, 42.8; HRMS (DART-TOF) m/z [M + H]$^+$ calculated for $C_{21}H_{23}BN_2O_5H$ = 394.1701, found = 394.1700.

*(2-((S)-3-((((9H-Fluoren-9-yl)methoxy)carbonyl)amino)-2-oxopyrrolidin-1-yl)-1-(4-fluorophenyl)ethyl)boronic Acid (**6f**).* Reference amount: 0.3 mmol, 155 mg. Light yellow solid; 41% yield. ^{1}H NMR (400 MHz, MeOD): δ 8.71 (s, 3H), 8.55−8.39 (m, 3H), 8.22−8.06 (m, 3H), 7.79−7.64 (m, 3H), 7.63−7.49 (m, 3H), 5.36 (s, 3H), 3.48−3.34 (m, 4H), 2.83 (s, 3H); ^{13}C NMR (126 MHz, CD_3OD): δ 141.8, 140.5, 140.0, 138.1, 136.1, 135.3, 134.6, 134.3, 56.7, 54.7, 46.2. HRMS (DART-TOF) m/z [M + H]$^+$ calculated for $C_{29}H_{30}BFN_2O_5H$ = 517.2218, found = 517.2215.

*((3,6-Dioxopiperazin-2-yl)methyl)boronic Acid (**8a**).* Reference amount: 0.1 mmol, 17 mg. White solid; 57% yield; ^{1}H NMR (400 MHz, MeOD): δ 4.43 (t, J = 6.6 Hz, 1H), 3.82 (dd, J = 7.7, 6.9 Hz, 1H), 3.69 (d, J = 17.1 Hz, 1H), 3.29 (d, J = 17.1 Hz, 1H), 2.98 (dd, J = 13.8, 6.9 Hz, 1H), 2.85−2.73 (m, 1H). ^{13}C{^{1}H} NMR (101 MHz, CD_3CN): δ 173.5, 63.3, 52.7, 46.5, 34.3; ^{11}B NMR (400 MHz, CD_3CN): δ 29.1; HRMS (DART-TOF) m/z [M + H]$^+$ calculated for $C_5H_9BN_2O_4H$ = 173.0711, found = 173.0710.

*((3,6-Dioxo-5-phenylpiperazin-2-yl)methyl)boronic Acid (**8b**).* *Single diastereomer characterized. Reference amount: 0.1 mmol, 25 mg. Light yellow solid; 62% yield; ^{1}H NMR (400 MHz, DMSO-d_6): δ 7.44−7.30 (m, 3H), 7.29−5.17 (m, 2H), 3.89 (dd, J = 11.7, 4.0 Hz, 1H), 3.81 (dd, J = 11.7, 3.3 Hz, 1H), 3.33−3.25 (s, 1H), 2.17 (t, J = 8.1 Hz, 1H); ^{13}C{^{1}H} NMR (126 MHz, MeOD): δ 168.0, 167.4, 132.9, 130.9, 129.5, 126.7, 124.0, 56.5, 54.7; ^{11}B NMR (400 MHz, CD_3CN): δ 30.1; HRMS (ESI+) [M + H$^+$] calculated for $C_{11}H_{13}BN_2O_4H$ = 249.1006, found = 249.1004.

*((5-Benzyl-3,6-dioxopiperazin-2-yl)methyl)boronic Acid (**8c**).* *Single diastereomer characterized. Reference amount: 0.1 mmol, 26 mg. Light yellow solid; 57% yield; ^{1}H NMR (400 MHz, MeOD): δ 7.43 (s, 2H), 7.28 (m, 3H), δ 4.43 (t, J = 6.6 Hz, 1H), 3.82 (dd, J = 7.7, 6.9 Hz, 1H), 3.69 (d, J = 17.1 Hz, 1H), 3.29 (d, J = 17.1 Hz, 1H), 2.98 (dd, J = 13.8, 6.9 Hz, 1H), 2.85−2.73 (m, 1H). ^{13}C{^{1}H} NMR (101 MHz, CD_3CN): δ 207.6, 135.4, 123.9, 118.3, 61.1, 30.9; ^{11}B NMR (400 MHz, CD_3CN): δ 32.3; HRMS (DART-TOF) m/z [M + H]$^+$ calculated for $C_{12}H_{15}BN_2O_4H$ = 263.1100, found = 263.1100.

*((1,4-Dioxooctahydropyrrolo[1,2-a]pyrazin-3-yl)methyl)boronic Acid (**8d**).* *Single diastereomer characterized. Reference amount: 0.1 mmol, 21 mg. Light yellow solid; 55% yield; ^{1}H NMR (400 MHz, DMSO-d_6): δ 2.05 (tt, J = 11.5, 3.2 Hz, 1H), 1.73−1.62 (m, 4H), 1.37−1.04 (m, 5H); ^{13}C{^{1}H} NMR (101 MHz, DMSO): δ 177.4, 43.7, 29.2, 25.5, 25.3; ^{11}B NMR (400 MHz, CD_3CN): δ 31.0; HRMS (DART-TOF) m/z [M + H]$^+$ calculated for $C_8H_{13}BN_2O_4H$ = 212.1001, found = 212.1008.

Biological Studies. Metallo-β-lactamase inhibitory activity was measured by monitoring the fluorescence after enzymatic hydrolysis of the cephalosporin reporter molecule FC5.[49] Clinically relevant metallo-β-lactamases (VIM-1, 500 pM; NDM-1, 20 pM; VIM-2, 100 pM; IMP-1, 20 pM) were incubated for 10 min with different concentrations of the inhibitors (100 μM−5 nM) in MBL buffer (50 mM HEPES, pH 7.2, 1 μM ZnSO4, 1 μg mL^{-1} BSA, 0.01% v/v Triton X-100). After incubation, the substrate FC5 (final concentration: 5 μM) was added and hydrolysis was recorded using a ClarioStar or PHERAstar FS microplate reader (BMG LabTech). Captopril, a known binder of metallo-β-lactamases, was used as a positive inhibitor control. Activity curves are located in the Supporting Information.

■ ASSOCIATED CONTENT

Supporting Information

The Supporting Information is available free of charge at https://pubs.acs.org/doi/10.1021/acs.joc.1c02015.

^{1}H NMR, ^{13}C NMR, and ^{11}B NMR spectra of synthesized compounds; computational data for mechanistic studies; and table and inhibition curves for biological studies (PDF)

■ AUTHOR INFORMATION

Corresponding Author

Andrei K. Yudin − *Department of Chemistry, University of Toronto, Toronto, ON M5S 3H6, Canada;* orcid.org/0000-0003-3170-9103; Email: andrei.yudin@utoronto.ca

Authors

Harjeet S. Soor − *Department of Chemistry, University of Toronto, Toronto, ON M5S 3H6, Canada*

Diego B. Diaz − *Department of Chemistry, University of Toronto, Toronto, ON M5S 3H6, Canada*

Ka Yi Tsui − *Department of Chemistry, University of California−Davis, Davis, California 95616, United States*

Karina Calvopiña − *Department of Chemistry and the Ineos Oxford Institute for Antimicrobial Research, University of Oxford, Oxford OX1 3TA, United Kingdom*

Marcin Bielinski − *Department of Chemistry and the Ineos Oxford Institute for Antimicrobial Research, University of Oxford, Oxford OX1 3TA, United Kingdom*

Dean J. Tantillo − *Department of Chemistry, University of California−Davis, Davis, California 95616, United States;* orcid.org/0000-0002-2992-8844

Christopher J. Schofield − *Department of Chemistry and the Ineos Oxford Institute for Antimicrobial Research, University of Oxford, Oxford OX1 3TA, United Kingdom;* orcid.org/0000-0002-0290-6565

Complete contact information is available at: https://pubs.acs.org/10.1021/acs.joc.1c02015

Author Contributions

The manuscript was written through contributions of all authors. All authors have given approval to the final version of the manuscript.

Notes

The authors declare no competing financial interest.

■ ACKNOWLEDGMENTS

We thank D. Burns and the CSICOMP NMR facility for assistance with spectroscopic experiments. The Natural Sciences and Engineering Research Council of Canada

(NSERC) is acknowledged for their financial support. The National Science Foundation (NSF) is acknowledged for their financial support (via CHE-1856416 and the XSEDE program). D.B.D. would like to thank NSERC for PGS D funding. K.C., M.B., and C.J.S. thank the E.P.S.R.C. Synthesis for Biology and Medicine Doctoral Training Center and the Medical Research Council for funding.

REFERENCES

(1) Diaz, D. B.; Yudin, A. K. The Versatility of Boron in Biological Target Engagement. *Nat. Chem.* **2017**, *9*, 731−742.
(2) Zhang, W.; Bryson, D. I.; Crumpton, J. B.; Wynn, J.; Santos, W. L. Branched Peptideboronic Acids (BPBAs): A Novel Mode of Binding Towards RNA. *Chem. Commun.* **2013**, *49*, 2436−2438.
(3) Hecker, S. J.; Reddy, K. R.; Totrov, M.; Hirst, G. C.; Lomovskaya, O.; Griffith, D. C.; King, P.; Tsivkovski, R.; Sun, D.; Sabet, M.; Tarazi, Z.; Clifton, M. C.; Atkins, K.; Raymond, A.; Potts, K. T.; Abendroth, J.; Boyer, S. H.; Loutit, J. S.; Morgan, E. E.; Durso, S.; Dudley, M. N. Discovery of a Cyclic Boronic Acid β-Lactamase Inhibitor (RPX7009) with Utility vs Class A Serine Carbapenemases. *J. Med. Chem.* **2015**, *58*, 3682−3692.
(4) Sharma, N.; Sharma, D. An Upcoming Drug for Onychomycosis: Tavaborole. *J. Pharmacol. Pharmacother.* **2015**, *6*, 236−239.
(5) Soor, H. S.; Hansen, J.; Diaz, D. B.; Appavoo, S.; Yudin, A. K. Solid-Phase Synthesis of Peptide β-Aminoboronic Acids. *Pept. Sci.* **2019**, *111*, No. e24072.
(6) Šterman, A.; Sosič, I.; Gobec, S.; Časar, Z. Synthesis of Aminoboronic Acid Derivatives: An Update on Recent Advances. *Org. Chem. Front.* **2019**, *6*, 2991−2998.
(7) Touchet, S.; Carreaux, F.; Carboni, B.; Bouillon, A.; Boucher, J.-L. Aminoboronic Acids and Esters: From Synthetic Challenges to the Discovery of Unique Classes of Enzyme Inhibitors. *Chem. Soc. Rev.* **2011**, *40*, 3895−3914.
(8) Robertson, N. S.; Spring, D. R. Using Peptidomimetics and Constrained Peptides as Valuable Tools for Inhibiting Protein-Protein Interactions. *Molecules* **2018**, *23*, 959.
(9) Hruby, V. J.; Li, G.; Haskell-Luevano, C.; Shenderovich, M. Design of Peptides, Proteins, and Peptidomimetics in Chi Space. *Biopolymers* **1997**, *43*, 219−266.
(10) Yudin, A. K. Macrocycles: Lessons from the Distant Past, Recent Developments, and Future Directions. *Chem. Sci.* **2015**, *6*, 30−49.
(11) Appavoo, S. D.; Kaji, T.; Frost, J. R.; Scully, C. C. G.; Yudin, A. K. Development of Endocyclic Control Elements for Peptide Macrocycles. *J. Am. Chem. Soc.* **2018**, *140*, 8763−8770.
(12) Kelly, T. A.; Fuchs, V. U.; Perry, C. W.; Snow, R. J. The Efficient Synthesis and Simple Resolution of a Prolineboronate Ester Suitable for Enzyme-Inhibition Studies. *Tetrahedron* **1993**, *49*, 1009−1016.
(13) Fawcett, A.; Pradeilles, J.; Wang, Y.; Mutsuga, T.; Myers, E. L.; Aggarwal, V. K. Photoinduced Decarboxylative Borylation of Carboxylic Acids. *Science* **2017**, *357*, 283−286.
(14) Lai, J. H.; Wu, W.; Zhou, Y.; Maw, H. H.; Liu, Y.; Milo, L. J.; Poplawski, S. E.; Henry, G. D.; Sudmeier, J. L.; Sanford, D. G.; Bachovchin, W. W. Synthesis and Characterization of Constrained Peptidomimetic Dipeptidyl Peptidase IV Inhibitors: Amino-Lactam BoroAlanines. *J. Med. Chem.* **2007**, *50*, 2391−2398.
(15) Hyland, S. N.; Meck, E. A.; Tortosa, M.; Clark, T. B. α-Amidoboronate Esters by Amide-Directed Alkane C−H Borylation. *Tetrahedron Lett.* **2019**, *60*, 1096−1098.
(16) Hennessy, E. J.; Saeh, J. C.; Sha, L.; MacIntyre, T.; Wang, H.; Larsen, N. A.; Aquila, B. M.; Ferguson, A. D.; Laing, N. M.; Omer, C. A. Discovery of Aminopiperidine-Based Smac Mimetics as IAP Antagonists. *Bioorg. Med. Chem. Lett.* **2012**, *22*, 1690−1694.
(17) Lima, L. M.; Alves, M. A.; do Amaral, D. N. Homologation: A Versatile Molecular Modification Strategy to Drug Discovery. *Curr. Top. Med. Chem.* **2019**, *19*, 1734−1750.
(18) Bolden, S., Jr.; Zhu, X. Y.; Etukala, J. R.; Boateng, C.; Mazu, T.; Flores-Rozas, H.; Jacob, M. R.; Khan, S. I.; Walker, L. A.; Ablordeppey, S. Y. Structure-Activity Relationship (SAR) and Preliminary Mode of Action Studies of 3-Substituted Benzylthioquinolinium Iodide as Anti-Opportunistic Infection Agents. *Eur. J. Med. Chem.* **2013**, *70*, 130−142.
(19) Lee, H. W.; Kim, H. O.; Choi, W. J.; Choi, S.; Lee, J. H.; Park, S. G.; Yoo, L.; Jacobson, K. A.; Jeong, L. S. Design, Synthesis, and Binding of Homologated Truncated 4′-Thioadenosine Derivatives at the Human A_3 Adenosine Receptors. *Bioorg. Med. Chem.* **2010**, *18*, 7015−7021.
(20) Adachi, S.; Cognetta, A. B.; Niphakis, M. J.; He, Z.; Zajdlik, A.; Denis, J. D. S.; Scully, C. C. G.; Cravatt, B. F.; Yudin, A. K. Facile Synthesis of Borofragments and their Evaluation in Activity-Based Protein Profiling. *Chem. Commun.* **2015**, *51*, 3608−3611.
(21) Diaz, D. B.; Scully, C. C. G.; Liew, S. K.; Adachi, S.; Trinchera, P.; St Denis, J. D.; Yudin, A. K. Synthesis of Aminoboronic Acid Derivatives from Amines and Amphoteric Boryl Carbonyl Compounds. *Angew. Chem., Int. Ed.* **2016**, *55*, 12849−12853.
(22) Tan, J.; Cognetta, A. B., III; Diaz, D. B.; Lum, K. M.; Adachi, S.; Kundu, S.; Cravatt, B. F.; Yudin, A. K. Multicomponent Mapping of Boron Chemotypes Furnishes Selective Enzyme Inhibitors. *Nat. Commun.* **2017**, *8*, 1760.
(23) Garrett, G. E.; Diaz, D. B.; Yudin, A. K.; Taylor, M. S. Reversible Covalent Interactions of β-Aminoboronic Acids with Carbohydrate Derivatives. *Chem. Commun.* **2017**, *53*, 1809−1812.
(24) Dawson, P. E.; Muir, T. W.; Clark-Lewis, I.; Kent, S. B. H. Synthesis of Proteins by Native Chemical Ligation. *Science* **1994**, *266*, 776−779.
(25) Aube, J.; Milligan, G. L. Intramolecular Schmidt Reaction of Alkyl Azides. *J. Am. Chem. Soc.* **1991**, *113*, 8965−8966.
(26) Reddy, D. S.; Judd, W. R.; Aubé, J. Lewis Acid-Mediated Reactions of Alkyl Azides with α,β-Unsaturated Ketones. *Org. Lett.* **2003**, *5*, 3899−3902.
(27) Charaschanya, M.; Aubé, J. Reagent-Controlled Regiodivergent Ring Expansions of Steroids. *Nat. Commun.* **2018**, *9*, 934.
(28) Diene, S. M.; Pinault, L.; Keshri, V.; Armstrong, N.; Khelaifia, S.; Chabrière, E.; Caetano-Anolles, G.; Colson, P.; La Scola, B.; Rolain, J.-M.; Pontarotti, P.; Raoult, D. Human Metallo-β-Lactamase Enzymes Degrade Penicillin. *Sci. Rep.* **2019**, *9*, 12173.
(29) Somboro, A. M.; Osei Sekyere, J.; Amoako, D. G.; Essack, S. Y.; Bester, L. A. Diversity and Proliferation of Metallo-β-Lactamases: a Clarion Call for Clinically Effective Metallo-β-Lactamase Inhibitors. *Appl. Environ. Microbiol.* **2018**, *84*, e00698−e00618.
(30) Brem, J.; Cain, R.; Cahill, S.; McDonough, M. A.; Clifton, I. J.; Jiménez-Castellanos, J.-C.; Avison, M. B.; Spencer, J.; Fishwick, C. W. G.; Schofield, C. J. Structural Basis of Metallo-β-Lactamase, Serine-β-Lactamase and Penicillin-Binding Protein Inhibition by Cyclic Boronates. *Nat. Commun.* **2016**, *7*, 12406.
(31) Clevenger, K. D.; Wu, R.; Liu, D.; Fast, W. n-Alkylboronic Acid Inhibitors Reveal Determinants of Ligand Specificity in the Quorum-Quenching and Siderophore Biosynthetic Enzyme PvdQ. *Biochemistry* **2014**, *53*, 6679−6686.
(32) Ishihara, K.; Ohara, S.; Yamamoto, H. Direct Polycondensation of Carboxylic Acids and Amines Catalyzed by 3,4,5-Trifluorophenylboronic Acid. *Macromolecules* **2000**, *33*, 3511−3513.
(33) Sabatini, M. T.; Boulton, L. T.; Sheppard, T. D. Borate Esters: Simple Catalysts for the Sustainable Synthesis of Complex Amides. *Sci. Adv.* **2017**, *3*, No. e1701028.
(34) Ishihara, K.; Ohara, S.; Yamamoto, H. 3,4,5-Trifluorobenzeneboronic Acid as an Extremely Active Amidation Catalyst. *J. Org. Chem.* **1996**, *61*, 4196−4197.
(35) Arnold, K.; Davies, B.; Giles, R. L.; Grosjean, C.; Smith, G. E.; Whiting, A. To Catalyze or not to Catalyze? Insight into Direct Amide Bond Formation from Amines and Carboxylic Acids under Thermal and Catalyzed Conditions. *Adv. Synth. Catal.* **2006**, *348*, 813−820.
(36) Gernigon, N.; Al-Zoubi, R. M.; Hall, D. G. Direct Amidation of Carboxylic Acids Catalyzed by *ortho*-Iodo Arylboronic Acids: Catalyst Optimization, Scope, and Preliminary Mechanistic Study Supporting a

https://doi.org/10.1021/acs.joc.1c02015
J. Org. Chem. 2022, 87, 94−102

Peculiar Halogen Acceleration Effect. *J. Org. Chem.* **2012**, *77*, 8386−8400.
(37) Bartoccini, F.; Bartolucci, S.; Lucarini, S.; Piersanti, G. Synthesis of Boron- and Silicon-Containing Amino Acids through Copper-Catalysed Conjugate Additions to Dehydroalanine Derivatives. *Eur. J. Org. Chem.* **2015**, *2015*, 3352−3360.
(38) *Gaussian 09*, Revision B. 01 Frisch, M. J.; Trucks, G. W.; Schlegel, H. B.; Scuseria, G. E.; Robb, M. A.; Cheeseman, J. R.; Scalmani, G.; Barone, V.; Petersson, G. A.; Nakatsuji, H.; Li, X.; Caricato, M.; Marenich, A. V.; Bloino, J.; Janesko, B. G.; Gomperts, R.; Mennucci, B.; Hratchian, H. P.; Ortiz, J. V.; Izmaylov, A. F.; Sonnenberg, J. L.; Williams-Young, D.; Ding, F.; Lipparini, F.; Egidi, F.; Goings, J.; Peng, B.; Petrone, A.; Henderson, T.; Ranasinghe, D.; Zakrzewski, V. G.; Gao, J.; Rega, N.; Zheng, G.; Liang, W.; Hada, M.; Ehara, M.; Toyota, K.; Fukuda, R.; Hasegawa, J.; Ishida, M.; Nakajima, T.; Honda, Y.; Kitao, O.; Nakai, H.; Vreven, T.; Throssell, K.; Montgomery, J. A., Jr.; Peralta, J. E.; Ogliaro, F.; Bearpark, M. J.; Heyd, J. J.; Brothers, E. N.; Kudin, K. N.; Staroverov, V. N.; Keith, T. A.; Kobayashi, R.; Normand, J.; Raghavachari, K.; Rendell, A. P.; Burant, J. C.; Iyengar, S. S.; Tomasi, J.; Cossi, M.; Millam, J. M.; Klene, M.; Adamo, C.; Cammi, R.; Ochterski, J. W.; Martin, R. L.; Morokuma, K.; Farkas, O.; Foresman, J. B.; Fox, D. J. Gaussian, Inc., Wallingford CT, 2009.
(39) (a) Tomasi, J.; Mennucci, B.; Cammi, R. Quantum Mechanical Continuum Solvation Models. *Chem. Rev.* **2005**, *105*, 2999−3094. (b) Leszczynski, J., Ed.; World Scientific Publishing Co. Pte. Ltd.: Singapore, 2003; Vol. *8*.
(40) (a) Becke, A. D. Density-Functional Thermochemistry. III. The Role of Exact Exchange. *J. Chem. Phys.* **1993**, *98*, 5648−5652. (b) Lee, C.; Yang, W.; Parr, R. G. Development of the Colle-Salvetti Correlation-Energy Formula into a Functional of the Electron Density. *Phys. Rev. B* **1988**, *37*, 785−789. (c) Miehlich, B.; Savin, A.; Stoll, H.; Preuss, H. Results Obtained with the Correlation Energy Density Functionals of Becke and Lee, Yang and Parr. *Chem. Phys. Lett.* **1989**, *157*, 200−206.
(41) Zhao, Y.; Truhlar, D. G. The M06 Suite of Density Functionals for Main Group Thermochemistry, Thermochemical Kinetics, Noncovalent Interactions, Excited States, and Transition Elements: Two New Functionals and Systematic Testing of Four M06-Class Functionals and 12 Other Functionals. *Theor. Chem. Acc.* **2008**, *120*, 215−241.
(42) Mardirossian, N.; Head-Gordon, M. ωB97X-V: A 10-Parameter, Range-Separated Hybrid, Generalized Gradient Approximation Density Functional with Nonlocal Correlation, Designed by a Survival-of-the-Fittest Strategy. *Phys. Chem. Chem. Phys.* **2014**, *16*, 9904−9924.
(43) (a) Gonzalez, C.; Schlegel, H. B. Reaction Path Following in Mass-Weighted Internal Coordinates. *J. Phys. Chem.* **1990**, *94*, 5523−5527. (b) Fukui, K. The Path of Chemical Reactions − the IRC Approach. *Acc. Chem. Res.* **1981**, *14*, 363−368.
(44) Spartan, Version10 (Wavefunction, Ind.: Irvine, CA, USA, **2010**).
(45) KINISOT, Rzepa, H. S. London, UK, **2015**.
(46) (a) Bigeleisen, J.; Mayer, M. G. Calculation of Equilibrium Constants for Isotopic Exchange Reactions. *J. Chem. Phys.* **1947**, *15*, 261−267. (b) Saunders, M.; Laidig, K. E.; Wolfsberg, M. Theoretical calculation of equilibrium isotope effects using ab initio force constants: application to NMR isotope perturbation studies. *J. Am. Chem. Soc.* **1989**, *111*, 8989−8994.
(47) Hughes, M. P.; Smith, B. D. Enhanced carboxylate binding using urea and amide-based receptors with internal Lewis acid coordination: A cooperative polarization effect. *J. Org. Chem.* **1997**, *62*, 4492−4499.
(48) Hall, D. G. Boronic Acid Catalysis. *Chem. Soc. Rev.* **2019**, *48*, 3475−3496.
(49) van Berkel, S. S.; Brem, J.; Rydzik, A. M.; Salimraj, R.; Cain, R.; Verma, A.; Owens, R. J.; Fishwick, C. W. G.; Spencer, J.; Schofield, C. J. Assay Platform for Clinically Relevant Metallo-β -Lactamases. *J. Med. Chem.* **2013**, *56*, 6945−6953.
(50) Smoum, R.; Rubinstein, A.; Dembitsky, V. M.; Srebnik, M. Boron Containing Compounds as Protease Inhibitors. *Chem. Rev.* **2012**, *112*, 4156−4220.
(51) Brem, J.; Van Berkel, S. S.; Aik, W.; Rydzik, A. M.; Avison, M. B.; Pettinati, I.; Umland, K. D.; Kawamura, A.; Spencer, J.; Claridge, T. D. W.; McDonough, M. A.; Schofield, C. J. Rhodanine hydrolysis leads to potent thioenolate mediated metallo-β-lactamase inhibition. *Nat. Chem.* **2014**, *6*, 1084−1090.
(52) Ghosh, A. K.; Brindisi, M. Organic Carbamates in Drug Design and Medicinal Chemistry. *J. Med. Chem.* **2015**, *58*, 2895−2940.
(53) De Paola, C. C.; Bennett, B.; Holz, R. C.; Ringe, D.; Petsko, G. A. 1-Butaneboronic Acid Binding to Aeromonas Proteolytica Aminopeptidase: A Case of Arrested Development. *Biochemistry* **1999**, *38*, 9048−9053.
(54) Brem, J.; van Berkel, S. S.; Zollman, D.; Lee, S. Y.; Gileadi, O.; McHugh, P. J.; Walsh, T. R.; McDonough, M. A.; Schofield, C. J. Structural Basis of Metallo-β-Lactamase Inhibition by Captopril Stereoisomers. *Antimicrob. Agents Chemother.* **2016**, *60*, 142−150.

https://doi.org/10.1021/acs.joc.1c02015
J. Org. Chem. 2022, 87, 94−102